Hindawi
Shock and Vibration
Volume 2019, Article ID 6326510, 11 pages
https://doi.org/10.1155/2019/6326510

Research Article

Research on the Resonance Characteristics of Rock under Harmonic Excitation

Siqi Li,[1] Shenglei Tian,[1] Wei Li,[1] Tie Yan,[1] and Fuqing Bi[2]

[1]*Institute of Petroleum Engineering, Northeast Petroleum University, Daqing 163318, Heilongjiang, China*
[2]*The Fifth Oil Production Plant of Daqing Oilfield, Daqing 163513, Heilongjiang, China*

Correspondence should be addressed to Wei Li; liwei_nepu@126.com

Received 1 July 2019; Accepted 17 July 2019; Published 6 August 2019

Academic Editor: Chengzhi Shi

In order to study the resonance characteristics of rock under harmonic excitation, two vibration models have been presented to estimate the natural frequency of rock encountered during the drilling. The first one is a developed single-DOF model which considers the properties and dimensions of the rock. The second one is a multi-DOF model based on the principle of least action. Subsequently, the modal characteristics, as well as the influence of excitation frequency, the mechanical properties, and dimensions of the rock on its resonance frequency, are analyzed by using FEM. Finally, the ultrasonic test on artificial sandstones and materials of drill tools are carried out indoor, and the FFT transform method is adopted to obtain their resonance frequencies. Based on the analysis undertaken, it can be concluded that the natural frequency of the rock increases with the change of vibration mode. For the same kind of rock, the resonance frequency is inversely proportional to mass, while for the different kinds of rocks, the mechanical parameters, such as density, elastic modulus, and Poisson's ratio, determine the resonance frequency of the rock together. Besides, the shape of the rock is also one of the main factors affecting its resonance frequency. At last, the theoretical research results are further verified by ultrasonic tests.

1. Introduction

It is well known that the resonance is a very common physical phenomenon in nature, and it can be observed in almost every field of engineering technology. Because of its severe damage effect, many engineering structures, machines, and equipment are designed to avoid the occurrence of resonance effect. However, resonance also has a positive side, and it is of great significance in some fields, for instance, musical instrument manufacturing, medical testing, and so on. Nowadays, a new drilling technology which also takes advantage of the damage characteristic of resonance has been proposed in the petroleum engineering, namely, Resonance Enhanced Drilling (RED). The main idea of this technology is that the bit, while rotating, applies a dynamic impacting force with an adjustable high frequency to the rock, so that makes the rock resonate to achieve rock fragmentation [1]. The RED technology can solve the common problems, such as slow rate of penetration and serious wear of drill bit, when drilling the deep and hard formations [2–4].

The key of the RED technology is to realize the rock resonance. At present, the studies on the rock resonance mainly include the following aspects. The basic characteristic parameters of the rock are tested based on the acoustic and electromagnetic resonance principles. More specifically, elastic modulus [5–7], compressibility, density [8], shear modulus, and damping ratio [9] of the rock can be obtained by resonance ultrasonic spectrum and the pore characteristics, saturation [10], and sediment characteristics [11] of the rock can be extracted by nuclear magnetic resonance technology. Besides, the resonance characteristics of various structures of rocks are identified and analyzed based on the principle of seismic resonance measurement so as to provide

a better guidance for environmental safety [12–14]. In addition, there are also a large number of studies on the transformation of pavements and other rock engineering structures by utilizing the destructive properties of resonance [15].

However, since the key to realizing of the RED technology is to determine the magnitude or the range of the resonance frequency of the rock so that the corresponding harmonic vibration impact can be exerted on the rock to achieve resonance fragmentation. Moreover, the rock encountered in drilling is relatively small comparing with the rock structures which are in the natural environment. Therefore, although many experts and scholars have conducted lots of relevant studies on the rock resonance [16–18], the existing research results are still not completely applicable to the field of drilling. So it is very necessary to carry out the research on the resonance characteristics of the rock encountered in the drilling field.

In this paper, aiming at the small rocks, a single-DOF model of natural frequency considering the properties and dimensions of the rock is developed. Then, based on the principle of least action, a multi-DOF model of natural frequency is proposed. Consequently, the main influencing factors which affect the resonance characteristics of the rock are determined. The rest of the paper is organized as follows. In Section 3, numerical simulations are carried out to analyze the influence of key factors on the resonance frequency of the rock. Then the ultrasonic test is conducted on the artificial sandstones and the materials of drill tool in Section 4 to verify the theoretical research results and explain the feasibility of RED technology.

2. Natural Frequency Models of the Rock

In this section, two vibration models considering the properties and dimensions of the rock are proposed to estimate its natural frequency.

2.1. A Single-DOF Model of Natural Frequency. The vibration system of the rock under the drill bit during drilling can be represented by a physical model as shown in Figure 1. The mass m which is a particle is an abstraction of inertia and the massless spring with stiffness k is an abstraction of elasticity in the rock vibration system.

According to the vibration theory [19], the natural frequency of the above system can be expressed as follows:

$$\omega_{\mathrm{n}} = \sqrt{\frac{k}{m}}. \tag{1}$$

Assuming that the rock is an elastic homogeneous medium, its stiffness can be obtained from the stiffness formula of elastic material, namely,

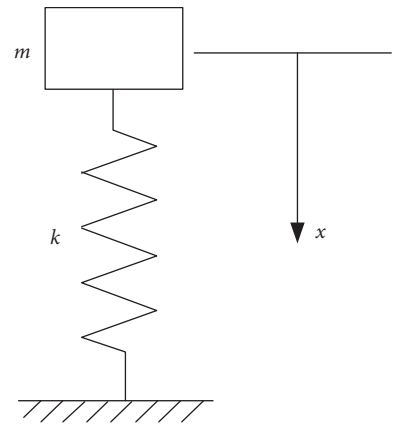

Figure 1: A single-DOF vibration model of the rock.

$$k = \frac{\mathrm{EA}}{l}. \tag{2}$$

Substituting equation (2) into equation (1), the natural frequency of the rock can be further rewritten as

$$\omega_{\mathrm{n}} = \sqrt{\frac{\mathrm{EA}}{ml}}, \tag{3}$$

or

$$f_{\mathrm{n}} = \frac{1}{2\pi}\sqrt{\frac{\mathrm{EA}}{ml}}. \tag{4}$$

Equation (4) is the single–DOF model of natural frequency of the rock.

2.2. A Multi-DOF Model of Natural Frequency. Due to the limitation of damping, energy, and other factors, the impact force of the drill bit can only pass a limited distance through the rock when drilling. As a result, the surface of the rock which is in contact with the drill bit breaks first. Therefore, the surface rock can be assumed as a homogeneous elastic plate comparing to the formation. Considering the actual situation of the rock at the bottom of the well, the plate is subjected to a simple support constraint, as shown in Figure 2.

Based on the principal of least action, the vibration equation of the above model can be given as

$$\rho u_{\mathrm{tt}} + \frac{D}{h}\Delta^2 u = 0. \tag{5}$$

Take the Fourier transform on the above equation, multiply both sides of the equation by $e^{i\omega t}$ and integrate. Then, equation (5) becomes

$$\rho\omega^2\tilde{u} + \frac{D}{h}\Delta^2\tilde{u} = 0. \tag{6}$$

Selecting the boundary of plate as the coordinate axis, the boundary condition can be expressed as

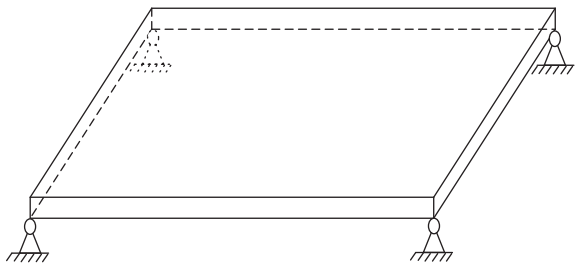

Figure 2: A multi-DOF vibration model of the rock.

$$u = 0,\ \frac{\partial^2 u}{\partial x^2} = 0, \quad x = 0, a,$$
$$u = 0,\ \frac{\partial^2 u}{\partial y^2} = 0, \quad y = 0, b. \tag{7}$$

The solution satisfying the above boundary conditions can be written as

$$u_0 = A \sin \frac{m\pi x}{a} \sin \frac{n\pi y}{b} \ (m \text{ and } n \text{ are integers}). \tag{8}$$

Thus, the natural frequency of the plate can be determined as

$$\omega_n = h\pi^2 \sqrt{\frac{E}{12\rho(1-\sigma^2)}} \left[\left(\frac{m}{a}\right)^2 + \left(\frac{n}{b}\right)^2 \right], \tag{9}$$

or

$$f_n = \frac{1}{2} h\pi \sqrt{\frac{E}{12\rho(1-\sigma^2)}} \left[\left(\frac{m}{a}\right)^2 + \left(\frac{n}{b}\right)^2 \right]. \tag{10}$$

Equation (10) is the multi-DOF model of natural frequency of the rock.

The above two vibration models can be used to estimate the natural frequency of the rock initially. Moreover, whether it is a single- or multi-DOF calculation model of natural frequency, we can find that the natural frequency of the rock is related to both its mechanical properties, such as stiffness, elastic modulus, Poisson's ratio, and density, and dimensions, such as length of side, area, and volume.

3. Numerical Simulation

In this section, modal analysis and harmonic response analysis are conducted to further study the resonance characteristics of rock. The modal analysis on the rock is to identify its natural frequency, while the harmonic response analysis is used to calculate the response frequency of the rock under a certain excitation frequency.

In the simulation, the shapes of rocks are block and cylinder and the lithologies of rocks are sandstone and granite. The models are intelligently meshed by tetrahedrons, as shown in Figure 3. The applied harmonic amplitude is 1000 N, and the impact frequencies are 10 kHz and 20 kHz, respectively. The specific properties of rocks are given in Table 1.

3.1. Modal Analysis. Figure 4 shows the natural frequencies of the first 30 orders of granite and sandstone with the size of 200 mm × 200 mm × 200 mm. It can be seen from the figure that the natural frequency of the rock increases with the change of the vibration mode and the rock has different resonance frequencies in different frequency ranges. Here, the natural frequency of sandstone is higher than that of granite in every order. According to the theoretical model, if the rock has the same shape, its natural frequency is proportional to elastic modulus and inversely proportional to Poisson's ratio and density. The results obtained from the simulation are consistent with the theoretical results.

3.2. Influence of Excitation Frequency. A harmonic impact force with the amplitude of 1000 N and the excitation frequency of 10 kHz and 20 kHz are exerted on the granite and sandstone with the dimension of 200 mm × 200 mm × 200 mm, respectively. The response results of rocks are shown in Figure 5. When the excitation frequency is within the range of 0~10 kHz, the resonance frequency of granite is 6900 Hz, and that of sandstone is 8700 Hz. However, when the excitation frequency is within the range of 0~20 kHz, the resonance frequencies of granite and sandstone are 10.6 kHz and 16.2 kHz, respectively. It can be seen that the resonance frequencies of the rock are different under different ranges of excitation frequency. As the excitation frequency increases, the resonance frequency of the rock also increases. It can be regarded as another manifestation that the rock has different natural frequencies for a multi-DOF system.

3.3. Influence of Mechanics Parameters of the Rock. The resonance frequencies curves of sandstone under a harmonic force of 1000 N and 20 kHz with the size of 100 mm × 100 mm × 100 mm, 200 mm × 200 mm × 200 mm, and 300 mm × 300 mm × 300 mm are presented in Figure 6(a). It can be seen that the bigger the rock is, the smaller the resonance frequency is when its mechanics parameters are the same. It could be also argued that the smaller the mass of the rock, the higher the frequency needed to make it resonate. Figure 6(b) depicts the resonance frequencies of granite and sandstone with the same volume and shape (200 mm × 200 mm × 200 mm) under a harmonic force of 1000 N and 20 kHz. Comparing the results presented in Figure 6(b), we note that the resonance frequency of granite is lower than that of sandstone. In the case of the same shape and size, the main factor that determines the resonance frequency of the rock is its mechanical properties. By comparing the density, elastic modulus, and Poisson's ratio of these two kinds of rocks, it can be found that the results of numerical simulation are consistent with the theoretical laws.

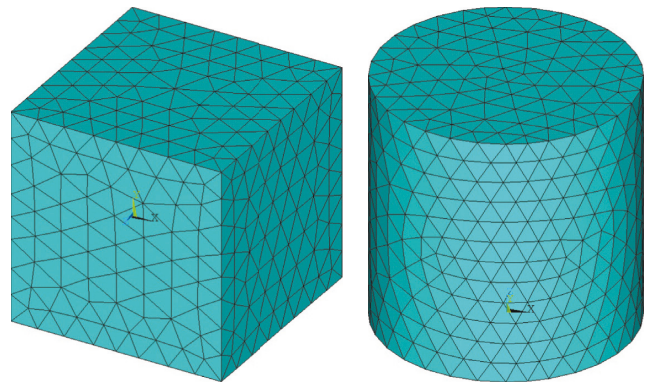

(a) (b)

Figure 3: Finite element models of rocks.

Table 1: Property parameters of rocks in the numerical simulation.

Lithology	Density Kg/m^3	Elastic modulus Pa	Poisson's ratio	Dimensions mm	
				Block	Cylinder
Granite	2790	2.6×10^{10}	0.26	$100\times100\times100$	$\Phi200\times200$
Sandstone	2560	4×10^{10}	0.34	$200\times200\times200$ $300\times300\times300$	$\Phi100\times200$

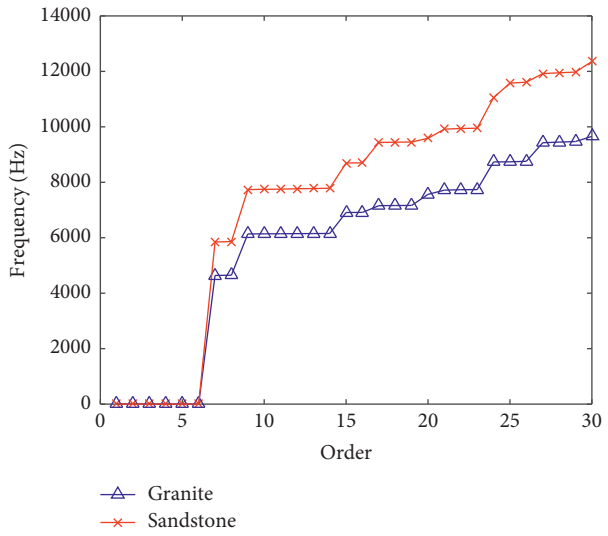

Figure 4: Modes in different orders of granite and sandstone.

3.4. Influence of the Shape of the Rock. Figure 7 plots the contrast curves of resonance frequencies of granite and sandstone with different shapes. Figure 7(a) shows harmonic response curves of cylindrical granite with the dimension of $\Phi100\,\text{mm}\times200\,\text{mm}$ ($v = 0.00157\,\text{m}^3$) and cubic granite with the size of $100\,\text{mm}\times100\,\text{mm}\times100\,\text{mm}$ ($v = 0.001\,\text{m}^3$). We can know from the simulation results that the resonance frequency of cylindrical granite is 14.4 kHz, and that of cubic granite is 10.6 kHz. It is obvious that the resonance frequency of the bigger cylindrical granite is higher than that of the smaller cubic granite. Similar analysis is performed on the sandstone, whose shapes are a cylinder with the dimension of $\Phi200\times200$ ($v = 0.00628\,\text{m}^3$) and a block with the size of $200\,\text{mm}\times200\,\text{mm}\times200\,\text{mm}$ ($v = 0.008\,\text{m}^3$), respectively. We can also get that the resonance frequency of cylindrical sandstone is 14.8 kHz and that of cubic sandstone is 16.2 kHz. It is evident from the presented results that the resonance frequency of the small cylindrical sandstone is lower than that of the big cubic sandstone.

Based on the single-DOF model, we can know that the rock with a small volume should have a large resonance frequency. However, the conclusion which we get from the simulation results is exactly opposite, which indicates that the shape of the rock does have an impact on its resonance frequency. The reason for this result may be due to that the stiffness of the rock will change with its shape, which will further affect its resonance frequency.

4. Ultrasonic Test

In order to further confirm the resonance characteristics of the rock, an indoor ultrasonic test on the resonance frequency of the rock is carried out.

4.1. Device and Cores. The device used in the test is an ultrasonic test system, which mainly includes an ultrasonic pulse generator/receiver, an oscilloscope, and low-frequency probes. The pulse generator/receiver has a frequency range

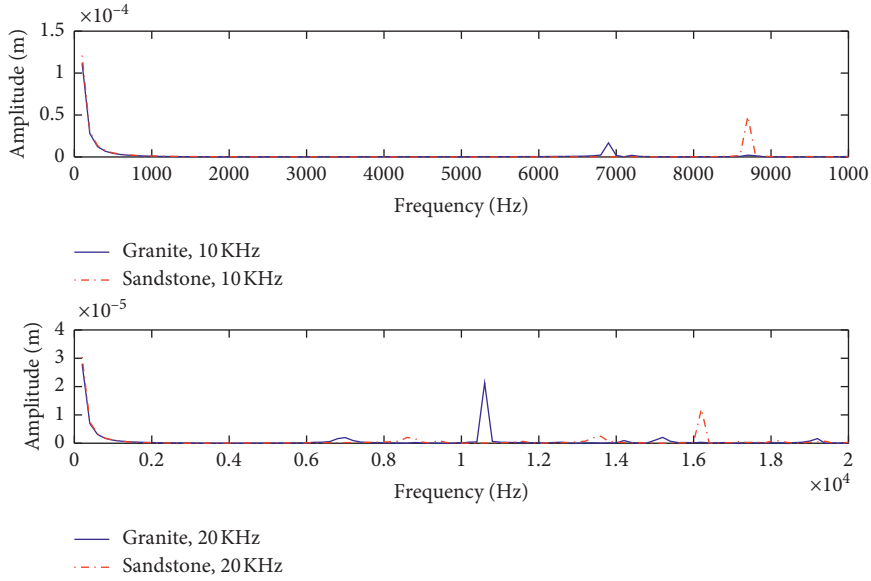

Figure 5: Resonance frequencies of granite and sandstone at different excitation frequencies.

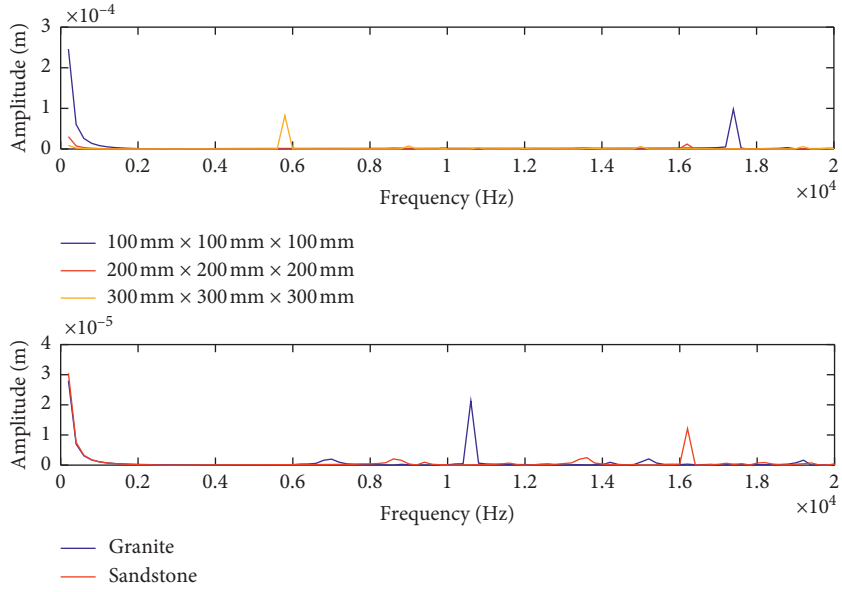

Figure 6: Resonance frequencies of rocks: (a) sandstones with the different volumes; (b) granite and sandstone with the same volume.

of 50 kHz to 20 MHz, and the frequencies of probe are 50 kHz and 250 kHz, respectively.

Artificial sandstone is used as the test core, and the mechanics parameters of rock have been given in the numerical simulation. The sandstone is processed into two shapes, which are cylinders with the sizes of Φ8 cm × 20 cm, Φ8 cm × 15 cm, Φ8 cm × 14 cm, Φ8 cm × 10 cm, Φ8 cm × 5 cm, and Φ8 cm × 3 cm and blocks with the sizes of 10 cm × 10 cm × 10 cm, 5 cm × 5 cm × 5 cm, and 4 cm × 4 cm × 4 cm, as shown in Figure 8.

4.2. Process and Principle. In the test, the pulse generator/receiver, the oscilloscope, and probes are connected as shown in Figure 9. The end face of the sandstone core should be flat, and the low-frequency probes are clamped at both ends of the core with butter as an adhesive.

The principle of the test is that a preset ultrasonic signal generated by the pulse generator/receiver device is applied to the sandstone core through a low-frequency probe. Here, the ultrasonic frequencies set in the test are 50 kHz and 250 kHz. Then, another low-frequency probe picks up the acoustic signal propagating from the core. At this time, the oscilloscope displays not only the transmitted signal, but also the acoustic signal received from the sandstone core. According to the received signal, the time-amplitude data of the rock can be obtained.

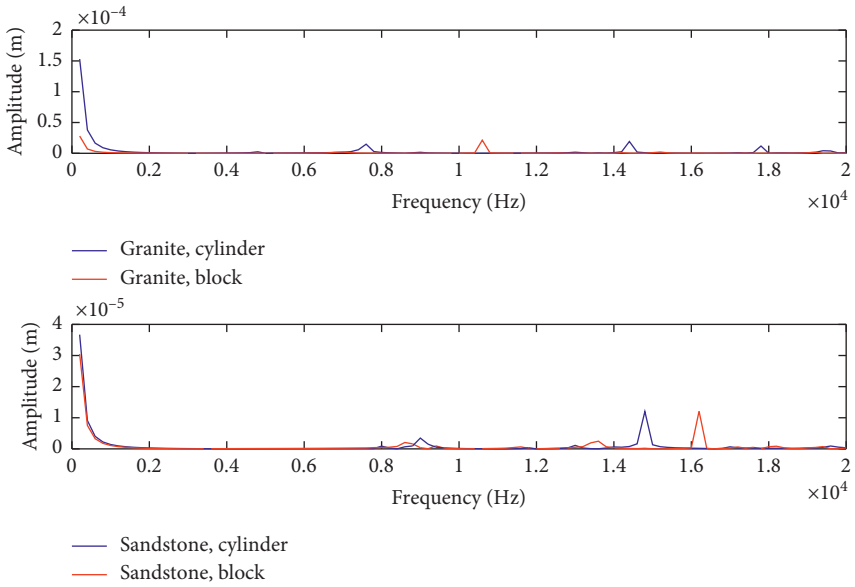

Figure 7: Resonance frequencies of different shapes of rocks: (a) granite; (b) sandstone.

Figure 8: Cores of artificial sandstone adopted in the test.

However, in order to obtain the resonance frequency of the core, it is necessary to perform FFT transformation on the time-amplitude curve and convert it into an amplitude-frequency curve, as shown in Figure 10. Then, the resonance frequency and maximum amplitude of the test core under a specific excitation frequency can be obtained, namley, the frequency and amplitude at the peak of the amplitude-frequency curve.

4.3. Experimental Results and Analysis. The resonance frequency and the maximum amplitude of the rock at the excitation frequencies of 50 kHz and 250 kHz can be obtained by processing the time-amplitude data. The experimental results are given in Table 2 and four representative amplitude-frequency curves are shown in Figure 11.

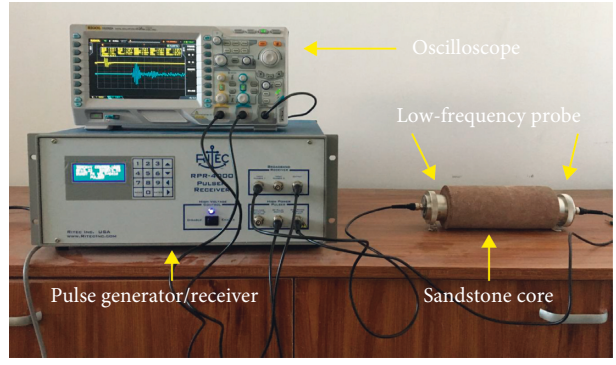

Figure 9: Schematic of the test device.

4.3.1. Influence of Excitation Frequency. The variation curves of resonance frequency of sandstone cores under the excitation frequencies of 50 kHz and 250 kHz are shown in Figure 12(a), and the enlarged resonance frequency curve under the excitation frequency of 50 kHz is given in Figure 12(b). Here, the cores 1 to 6 are cylindrical sandstones, and the cores 7 to 9 are cubic sandstones. It can be seen from the figure that the resonance frequencies of the same sandstone core are not the same under the different excitation frequencies, which increase with the increasing of the excitation frequency. The experimental results further verify the conclusion of the theoretical research.

4.3.2. Influence of Core Volume. Figure 13 shows the variation of the resonance frequencies of sandstone cores with different volumes under the excitation frequencies of 50 kHz and 250 kHz. It should be noted that the nine cores are arranged by volumes and do not distinguish their shapes. It can be seen from both of the two curves that as the core volume increases, the resonance frequency of the core basically

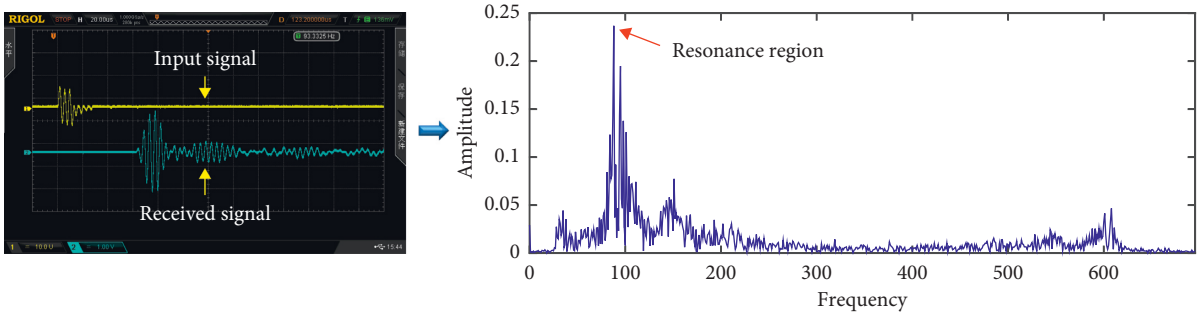

Figure 10: Signal processing of ultrasonic test.

Table 2: Ultrasonic test results of sandstone cores.

No.	Shape	Size	Resonance frequency (50 kHz) kHz	Amplitude	Resonance frequency (250 kHz) kHz	Amplitude
1	Cylinder	Φ8 cm × 20 cm	62	0.1691	92	0.1763
2		Φ8 cm × 15 cm	63	0.1438	92	0.2845
3		Φ8 cm × 14 cm	67	0.1874	93	0.317
4		Φ8 cm × 10 cm	67	0.1781	93	0.4409
5		Φ8 cm × 5 cm	68	0.4277	204	0.1986
6		Φ8 cm × 3 cm	68	0.4953	204	0.1611
7	Block	10 cm × 10 cm × 10 cm	63	0.5264	186	0.1368
8		5 cm × 5 cm × 5 cm	67	0.6015	197	0.1657
9		4 cm × 4 cm × 4 cm	68	0.4888	206	0.1347

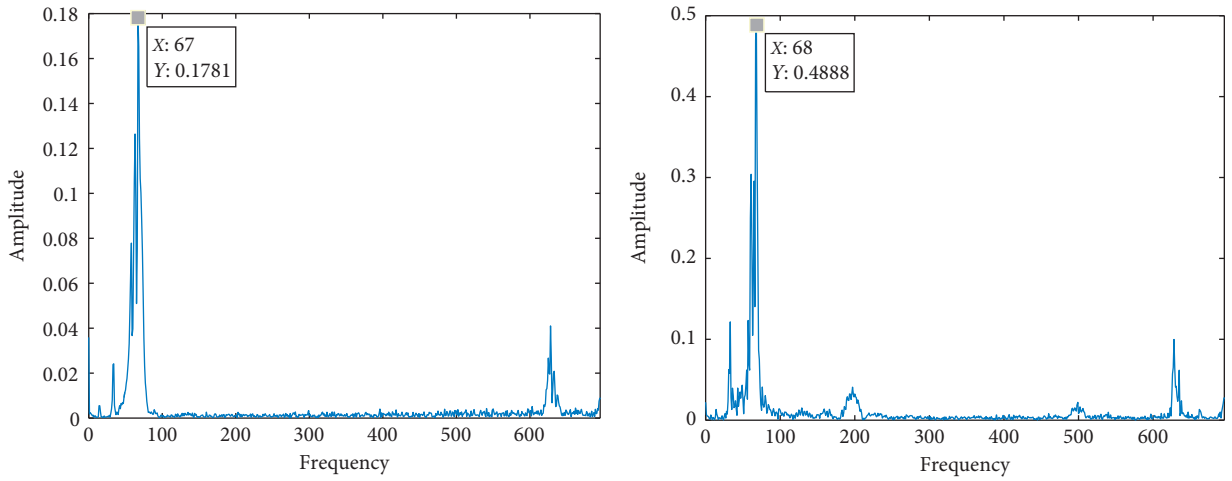

(a) (b)

Figure 11: Continued.

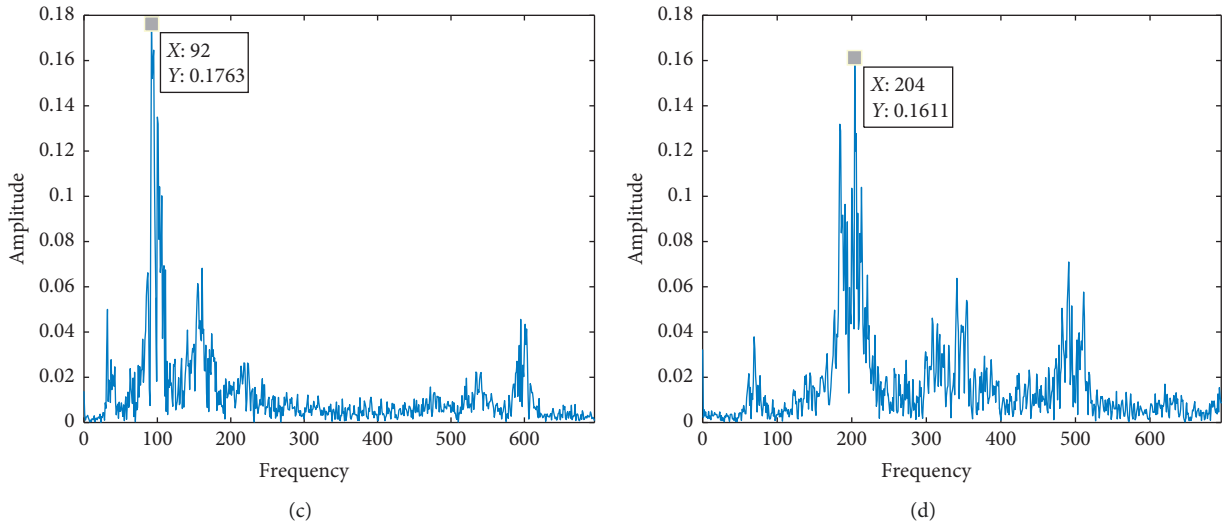

Figure 11: Representative amplitude-frequency curves of sandstones.

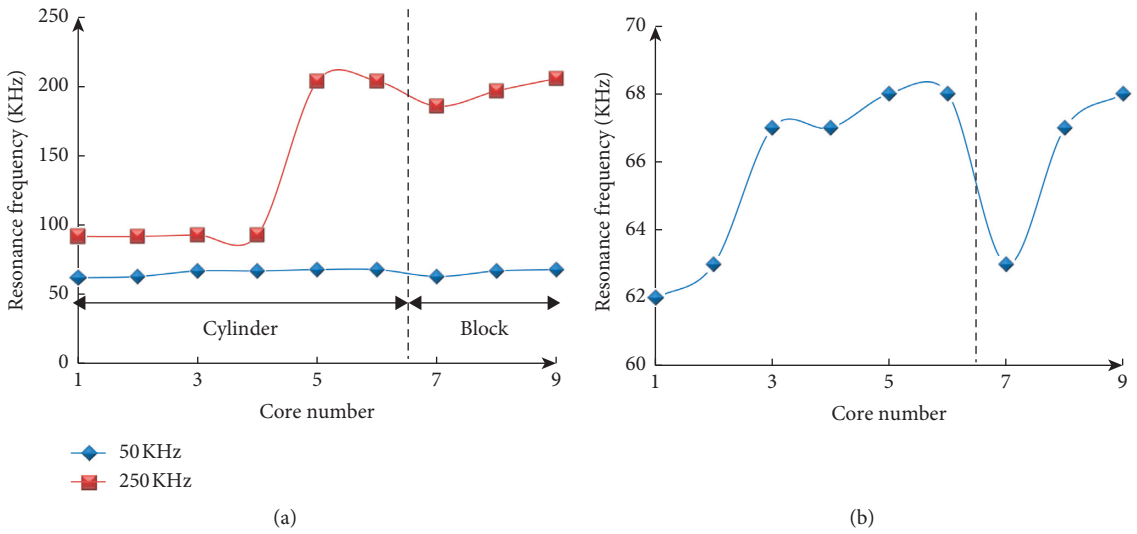

Figure 12: Resonance frequencies curves of sandstone cores under the different excitation frequencies: (a) the excitation frequency of 50 kHz and 250 kHz; (b) the excitation frequency of 50 kHz.

decreases. In addition, there is a singularity on the curve, which is caused by the different shapes of rocks. It can be confirmed by the curves of resonance frequency in Figure 12(b), where the volume of cylindrical sandstone decreases from 1 to 6 and the volume of cubic sandstone decreases from 7 to 9. Then, we can conclude that the resonance frequencies of cylindrical and cubic sandstone increase with the decreasing of their volumes under the two excitation frequencies.

Since the artificial sandstone core is homogeneous, its properties such as density can be considered the same. So when we do the qualitative analysis, the variable of core volume can be equivalent to the variable of core mass. Thus, it can be concluded that the larger the mass of the rock is, the lower its resonance frequency is, which agrees with the analysis of the theoretical model of the natural frequency of the rock.

4.3.3. Influence of Core Shape. The resonance frequencies of cylindrical and cubic sandstone cores with similar volumes are compared, as shown in Figure 14. As can be seen from the histogram, whether at the excitation frequency of 50 kHz (Figure 14(a)) or 250 kHz (Figure 14(b)), the resonance frequencies of big sandstone cores are higher than those of small sandstone cores. This

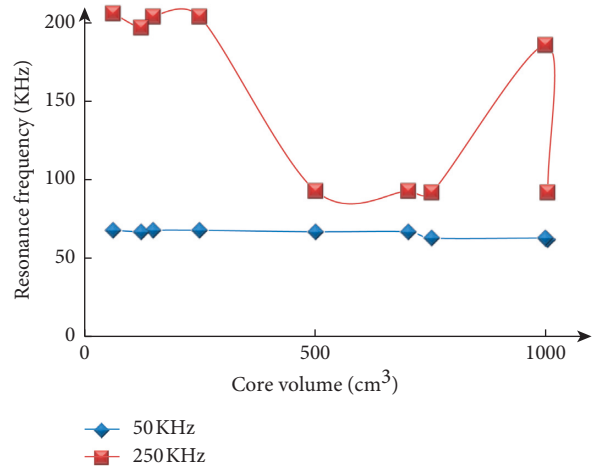

Figure 13: Relation curves of resonance frequency and volume of sandstone cores.

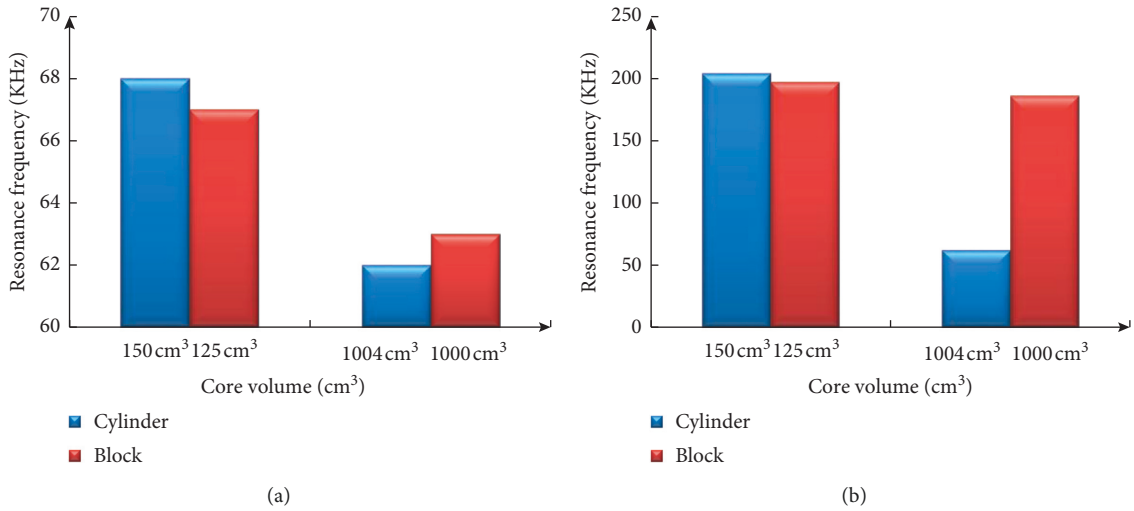

Figure 14: Histograms of resonance frequencies of sandstone cores with different shapes: (a) 50 kHz; (b) 250 kHz.

contradicts the previous conclusion that the resonance frequency of the rock with the same mechanics parameters is inversely proportional to its volume, which further verifies the conclusion that the shape of rock will affect its resonance frequency.

4.3.4. Comparison of Resonance Frequency between Rock and Drilling Tool. To ensure the feasibility of RED technology, it is important to find out whether the excitation frequency that causes the rock to resonate will damage the drilling tool. Therefore, a series of resonance frequency tests have been also carried out on the alloy steel used in drilling tools and the tungsten carbide used in cutting teeth of drill bit, and the comparison results are given in Figure 15.

Figure 15 shows the resonance frequency curves of rock, tungsten carbide, and alloy steel obtained at the excitation frequency of 50 kHz, respectively. It can be seen from the results that the resonance frequencies of tungsten carbide and rock are quite different, and the resonance frequencies of rock and alloy steel are relatively close. However, this is also related to the size of the test materials. In fact, to prevent high-frequency vibration from affecting the drill string system, the vibration isolation device needs to be installed between the RED module and the drill string to ensure that the drill string is not affected. Thus, even when resonance Thus, even if resonance frequencies of the alloy steel in drill string and the rock are similar, the drill tools will not be damaged during rock resonance.

5. Conclusions

In this paper, the resonance characteristics of the rock encountered during the drilling under harmonic excitation have been investigated theoretically and experimentally. Two vibration models of the rock which can be used to estimate its natural frequency have been presented. Firstly, a single-DOF model considering the properties and dimensions of the rock is developed. Then, a multi-DOF model is proposed based on the principle of least action. As a result, we can conclude that the resonance characteristics

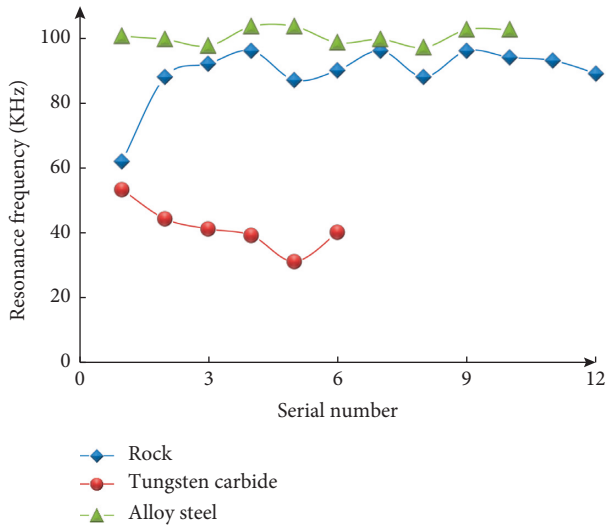

Figure 15: Comparison curves of resonance frequencies for rock and drilling tool.

of the rock are related to both its mechanical properties and dimensions.

The numerical simulations have been carried out to analyze the resonance characteristics of the rock. It can be known from the modal analysis that the natural frequency of the rock increases with the change of vibration mode, and the rock has different resonance frequencies in different frequency ranges. Besides, the harmonic response analysis shows that the resonance frequency of the rock increases with the increase of excitation frequency. For the same kind of rock, the smaller the mass is, the larger the resonance frequency is, while for the different kinds of rocks, the mechanical parameters such as density, elastic modulus, and Poisson's ratio determine the resonance frequency. Furthermore, the shape of the rock is also one of the main factors affecting the resonance frequency.

Finally, indoor tests have been conducted on artificial sandstones and materials of drill tools by an ultrasonic test system. The results obtained from the tests further verify the correctness of the theoretical analysis and explain the feasibility of RED technology.

Nomenclature

k: Stiffness of rock, N/m
m: Mass of rock, kg
l: Length of rock, m
E: Elastic modulus, MPa
A: Cross-sectional area of rock, m^2
ω_n: Natural angular frequency of rock, rad/s
f_n: Natural frequency of rock, Hz
ρ: Density of plate, kg/m^3
u: Vertical displacement of a point on a neutral plane, m
u_{tt}: Acceleration of plate, m/s^2
D: Bending rigidity of plate, $N{\cdot}m^2$
h: Thickness of plate, m
μ: Poisson's ratio
a, b: Length of plate, m.

Data Availability

The experimental data used to support the findings of this study are included within the article. There are no restrictions on data use.

Conflicts of Interest

The authors declare that they have no conflicts of interest.

Acknowledgments

The support of the National Natural Science Foundation of China (no. 51704074) and Youth Science Foundation of Heilongjiang Province (no. QC2018049) are gratefully acknowledged. The work is also supported by Talent Cultivation Foundation (nos. SCXHB201703, ts26180119, and td26180141) and Youth Science Foundation (no. 2019QNL-07) of Northeast Petroleum University.

References

[1] M. Wiercigroch, V. Vaziri, and M. Kapitaniak, "RED: revolutionary drilling technology for hard rock formations," in *Proceedings of the SPE/IADC Drilling Conference and Exhibition*, The Hague, The Netherlands, March 2017.

[2] H. Wang, G. Li, Z. Shen et al., "Experiment on rock breaking with supercritical carbon dioxide jet," *Journal of Petroleum Science and Engineering*, vol. 127, pp. 305–310, 2015.

[3] H. Wang, G. Li, Z. He et al., "Experimental investigation on abrasive supercritical CO_2 jet perforation," *Journal of CO_2 Utilization*, vol. 28, pp. 59–65, 2018.

[4] Y. Li, D. Jia, Z. Rui, J. Peng, C. Fu, and J. Zhang, "Evaluation method of rock brittleness based on statistical constitutive relations for rock damage," *Journal of Petroleum Science and Engineering*, vol. 153, no. 5, pp. 123–132, 2017.

[5] C. S. Park, I. B. Park, and Y. J. Mok, "Evaluation of resilient moduli for recycled crushed-rock-soil-mixtures using in-situ seismic techniques and large-scale resonant column tests," *KSCE Journal of Civil Engineering*, vol. 19, no. 6, pp. 1647–1655, 2015.

[6] B. Sandra, R. Patrick, D. S Noalwenn, V. Vassil, V. Poitrineau, and J.-F. Nauroy, "From noise correlation to resonant ultrasound spectroscopy in rock acoustics," *Geophysical Prospecting*, vol. 64, no. 5, pp. 1368–1385, 2016.

[7] T. J. Ulrich, K. R. McCall, and R. A. Guyer, "Determination of elastic moduli of rock samples using resonant ultrasound spectroscopy," *The Journal of the Acoustical Society of America*, vol. 111, no. 4, pp. 1667–1674, 2002.

[8] J. Zhao, G. Tang, J. Deng, X. Tong, and S. Wang, "Determination of rock acoustic properties at low frequency: a differential acoustical resonance spectroscopy device and its estimation technique," *Geophysical Research Letters*, vol. 40, no. 12, pp. 2975–2982, 2013.

[9] A. Perino and G. Barla, "Resonant column apparatus tests on intact and jointed rock specimens with numerical modelling

validation," *Rock Mechanics and Rock Engineering*, vol. 48, no. 1, pp. 197–211, 2015.

[10] C. H. Arns, T. A. Ghamdi, and J.-Y. Arns, "Numerical analysis of nuclear magnetic resonance relaxation–diffusion responses of sedimentary rock," *New Journal of Physics*, vol. 13, no. 1, article 015004, 2011.

[11] K. Jessica, U. J. van Raden, I. García-Rubio, and A. U. Gehring, "Rock magnetic techniques complemented by ferromagnetic resonance spectroscopy to analyse a sediment record," *Geophysical Journal International*, vol. 191, no. 1, pp. 51–63, 2012.

[12] Y. G. Fang and H. Cao, "Resonant property and catastrophe analyses of seismic response of multi-degree-of-freedom nonlinear structure," *Earthquake Engineering and Engineer Vibration*, vol. 23, no. 5, pp. 69–74, 2003.

[13] J. R. Moore, M. S. Thorne, K. D. Koper et al., "Anthropogenic sources stimulate resonance of a natural rock bridge," *Geophysical Research Letters*, vol. 43, no. 18, pp. 9669–9676, 2016.

[14] A. M. Starr, J. R. Moore, and M. S. Thorne, "Ambient resonance of mesa arch, canyonlands national park, Utah," *Geophysical Research Letters*, vol. 42, no. 16, pp. 6696–6702, 2015.

[15] X. Y. Wang, "The research on pavement structure mechanical behavior based on high frequency and low amplitude resonance crushing technology,"Doctoral dissertation, Chongqing Jiaotong University, Chongqing, China, 2013.

[16] E. Pavlovskaia, D. C. Hendry, and M. Wiercigroch, "Modelling of high frequency vibro-impact drilling," *International Journal of Mechanical Sciences*, vol. 91, pp. 110–119, 2015.

[17] M. Wiercigroch, A. M. Krivtsov, and J. Wojewoda, "Vibrational energy transfer via modulated impacts for percussive drilling," *Journal of Theoretical and Applied Mechanics*, vol. 46, no. 3, pp. 715–726, 2008.

[18] Q. Xue, H. Leung, L. Huang et al., "Modeling of torsional oscillation of drillstring dynamics," *Nonlinear Dynamics*, vol. 96, no. 1, pp. 267–283, 2019.

[19] W. T. Thomson, *Theory of Vibration with Applications*, Taylor & Francis, London, UK, 1993.